



Retrieval of Turbidity in Upper Lake, a Ramsar Site in Bhopal, India, Using *In Situ* Observations and Landsat 8 OLI Satellite Data

Prasanta Ghadei¹ and Sujit Kumar Jally^{1*}

School of Geography, Gangadhar Meher University, Sambalpur-768004, Odisha, India

*Corresponding author: Sujit Kumar Jally; sujit@gmuniversity.ac.in

Abbreviation: Nat. Env. & Poll. Technol.

Website: www.neptjournal.com

Received: 30-09-2025

Revised: 25-11-2025

Accepted: 27-11-2025

Key Words:

Empirical model
Landsat-8 OLI
Surface reflectance
Ramsar site
Turbidity
Upper Lake

Citation for the Paper:

Ghadei, P. and Jally, S.K., 2026. Retrieval of turbidity of the Upper Lake, a Ramsar site in Bhopal, India, using in-situ observations and Landsat-8 OLI satellite data. *Nature Environment and Pollution Technology*, 25(3), B4393. <https://doi.org/10.46488/NEPT.2026.v25i03.B4393>

Note: From 2025, the journal has adopted the use of Article IDs in citations instead of traditional consecutive page numbers. Each article is now given individual page ranges starting from page 1.



Copyright: © 2026 by the authors

Licensee: Technoscience Publications

This article is an open access article distributed under the terms and conditions of the Creative Commons Attribution (CC BY) license (<https://creativecommons.org/licenses/by/4.0/>).

ABSTRACT

Turbidity, an optical measure of water clarity influenced by suspended sediments and organic matter, is a critical indicator of freshwater quality. Satellite remote sensing offers a practical means of monitoring turbidity over space and time by capturing water-leaving reflectance across spectral bands. This study explores the spatiotemporal retrieval of turbidity in the Upper Lake, Bhopal, an important urban freshwater body and Ramsar site in India, using Landsat-8 Operational Land Imager (OLI) Surface Reflectance (SR) data from 2013 to 2022. Field-based in-situ turbidity data collected during the pre-monsoon and post-monsoon seasons of 2022 were used to calibrate and validate several empirical models based on different band combinations. The best empirical models used the band ratio of the blue and red bands (Band-2 and Band-4), yielding a high agreement with field data ($R^2 = 0.89$) with a validation RMSE of 4.04 NTU. Temporal turbidity trends revealed a seasonal pattern, with higher turbidity observed in the post-monsoon season due to catchment runoff and anthropogenic activities. This study confirmed that Landsat-8 OLI SR, supported by field measurements, is a reliable tool for long-term turbidity monitoring in inland lakes.

1. INTRODUCTION

Freshwater lakes and reservoirs are critical components of the Earth's hydrological cycle and provide a wide range of ecosystem services, including drinking water supply, irrigation, fisheries, biodiversity conservation, recreation, and climate regulation. However, in recent decades, many of these water bodies have faced significant degradation owing to anthropogenic pressures such as urbanization, agricultural runoff, industrial discharge, and climate change (UNESCO 2018). Among the various water quality parameters used to monitor aquatic ecosystem health, turbidity stands out as a key indicator because of its direct link with suspended sediment load, light attenuation, and pollutant transport (Das et al. 2024). Turbidity refers to the degree to which water loses its transparency owing to the presence of suspended particulates, such as silt, clay, organic matter, plankton, and microorganisms. It affects aquatic life by reducing sunlight penetration, which limits photosynthetic activity in submerged vegetation and algae (Bilotta & Brazier 2008). High turbidity levels also interfere with the reproduction and feeding behavior of aquatic organisms and can carry attached contaminants, such as heavy metals and pathogens, posing risks to both ecosystems and public health (Chen & Chen 2017). Therefore, understanding the spatial and temporal patterns of lake turbidity is essential for water quality management and policy formulation.

Traditionally, turbidity is measured using in-situ techniques, such as Secchi disk readings and nephelometric turbidity units (NTU) using turbidity meters. Although accurate at specific points, these methods are inherently limited in their ability to capture spatial variability across an entire water body, especially large or remote lakes. Moreover, repeated sampling at high temporal frequencies is often cost-prohibitive and labor-intensive (Dekker et al. 2002). This necessitates the use

of alternative, scalable approaches for monitoring turbidity, particularly in regions such as India, where resource constraints limit large-scale water quality monitoring. Remote sensing has emerged as a promising solution to address these challenges. Satellite-based sensors provide consistent, synoptic, and long-term observations of surface reflectance that can be used to estimate various water quality parameters, including turbidity (Jally et al. 2021). In recent years, the Landsat-8 Operational Land Imager (OLI) has gained popularity owing to its moderate spatial resolution (30 m), improved radiometric sensitivity, and free availability through the USGS Earth Explorer platform. The Surface Reflectance (SR) product, which accounts for atmospheric distortions, is particularly well-suited for quantitative water quality assessments (Pahlevan et al. 2017, Brezonik et al. 2005). Numerous studies have demonstrated the feasibility of retrieving turbidity from Landsat data using empirical relationships between spectral reflectance and turbidity values. The blue (Band-2), green (Band-3), and red (Band-4) bands are commonly the most responsive to increases in suspended matter because of their interaction with particulate matter in the water column (Maity et al. 2022, Wen et al. 2022). Empirical regression models, band ratio techniques, and semi-analytical models have been successfully employed to map turbidity in a range of aquatic environments, from rivers and estuaries to lakes and wetlands. These models are typically calibrated with field-measured turbidity values and validated using statistical indices such as the coefficient of determination (R^2), root mean square error (RMSE), and mean absolute percentage error (MAPE) (Yang et al. 2022).

In India, the application of remote sensing for inland water quality monitoring is still emerging but holds immense potential. The country's vast network of rivers, lakes, and reservoirs is under increasing stress owing to population growth, urban sprawl, and insufficient wastewater treatment infrastructure. One such water body is the Upper Lake (Bhojtal) in Bhopal, Madhya Pradesh, India. This ancient man-made lake, created in the 11th century, serves as the primary drinking water source for nearly 1.5 million people and supports significant biodiversity. Designated as a Ramsar site in 2002, the Upper Lake is recognized for its ecological and socioeconomic importance. However, it faces growing threats from untreated sewage inflow, agricultural runoff, eutrophication, encroachment, and climate variability (CPCB 2019). Given the environmental importance of Upper Lake, Bhopal, and the lack of continuous water quality monitoring data, there is a pressing need to develop and apply satellite-based approaches to assess its turbidity levels over time. The present study aims to address this gap by retrieving turbidity across a spatiotemporal scale (2013–2022) using Landsat-8 OLI SR data in conjunction with *in situ* turbidity

measurements. The objective of this study was to develop and validate turbidity retrieval algorithms using Landsat-8 OLI SR data and *in-situ* field observations, thereby producing seasonal turbidity maps from 2013 to 2022. The results are expected to assist policymakers and lake managers in better understanding turbidity dynamics and in implementing appropriate conservation strategies. This study contributes to the growing body of knowledge on remote sensing applications in inland water quality monitoring and provides a replicable framework for similar studies in other Indian and global lakes under environmental stress.

2. MATERIALS AND METHODS

2.1 Study Area

The Upper Lake, locally known as Bhojtal, is one of the most prominent freshwater lakes in Central India. It is situated in the western part of Bhopal, the capital city of Madhya Pradesh, and forms a vital part of the city's ecological and socioeconomic landscape (Fig. 1). This ancient lake, believed to have been constructed in the 11th century by King Raja Bhoj, is among the oldest man-made lakes in India and is intricately linked to the cultural and historical heritage of the region (Everard et al. 2020). Geographically, the lake lies between $23^{\circ}12'$ and $23^{\circ}16'$ N latitude and $77^{\circ}18'$ and $77^{\circ}22'$ E longitude, with an average altitude of approximately 500 m above sea level. The Upper Lake spans a surface area of approximately 31 square kilometers and is part of the larger Bhoj Wetland system, which also includes the adjoining Lower Lake. Together, these wetlands were designated as Ramsar sites in 2002 under the Convention on Wetlands of International Importance, highlighting their ecological significance and the need for conservation (Ramsar Sites Information Service 2024). It is primarily fed by rainfall and surface runoff from a catchment area of nearly 361 square kilometers, which consists of forested hills, agricultural lands, and urban settlements. The Kolans River, a seasonal tributary, also contributes to lake inflow. The lake is the main drinking water source for more than 1.5 million residents of Bhopal and supports domestic, agricultural, and recreational activities. In addition to its economic and utilitarian roles, the lake provides a habitat for a diverse range of aquatic flora and fauna, including migratory bird species such as bar-headed geese, black-winged stilts, and cormorants (Rather & Gautam 2023). The region experiences a tropical wet and dry climate, characterized by three major seasons: summer (March–June), monsoon (July–September), and winter (October–February). The average annual rainfall is approximately 1200 mm, with the majority of precipitation occurring during the monsoon

months. This seasonal rainfall pattern plays a significant role in influencing the hydrological and sediment dynamics of the lake, thereby affecting the turbidity levels. During the monsoon, increased surface runoff brings suspended sediments, nutrients, and organic matter into lakes, often leading to elevated turbidity and eutrophication, particularly near urban and agricultural inflow points (Parashar et al. 2008). In this study, the lake was categorized into three sectors based on Secchi disk transparency, nutrients, and depth: western (WS), central (CS), and eastern (ES) sectors for the ecological assessment.

2.2 Database and Methodology

This study integrated field-based turbidity measurements with satellite remote sensing data from the Landsat-8 Operational Land Imager (OLI) to develop an empirical model for turbidity retrieval. The methodology was carefully structured to ensure the accuracy of the calibration, validation, and application of the model across a spatiotemporal scale. The process comprised in-situ data collection, satellite image selection and preprocessing, band ratio analysis, model development, and the generation of seasonal turbidity maps for the pre-monsoon and post-monsoon seasons from 2013 to 2022 (Fig. 3). All data were analyzed using a

combination of Remote Sensing, GIS, and statistical software to enable high-resolution spatial analysis and trend interpretation.

2.2.1 Turbidity Data Collection

Fieldwork was conducted during the pre- and post-monsoon seasons of 2022. A total of 50 sampling locations were selected within the Upper Lake. At each location, turbidity was measured using a portable HANNA HI-98703 turbidity meter, which operates based on nephelometric principles that conform to ISO 7027 standards. To minimize variability, three consecutive readings were taken at each site, and the average value was recorded in Nephelometric Turbidity Units (NTU). Simultaneously, the geographic coordinates of each point were recorded using a Garmin GPSMAP 64s handheld device to ensure accurate geospatial alignment with the satellite pixels.

2.2.2 Acquisition of Satellite Data

The satellite data used in this study consisted of Landsat-8 Surface Reflectance (SR) imagery, which was atmospherically corrected and available via the USGS Earth Explorer portal. Landsat-8 OLI provides multispectral imagery at 30-meter resolution, making it highly suitable for monitoring medium-scale inland water bodies such as the Upper Lake. For each

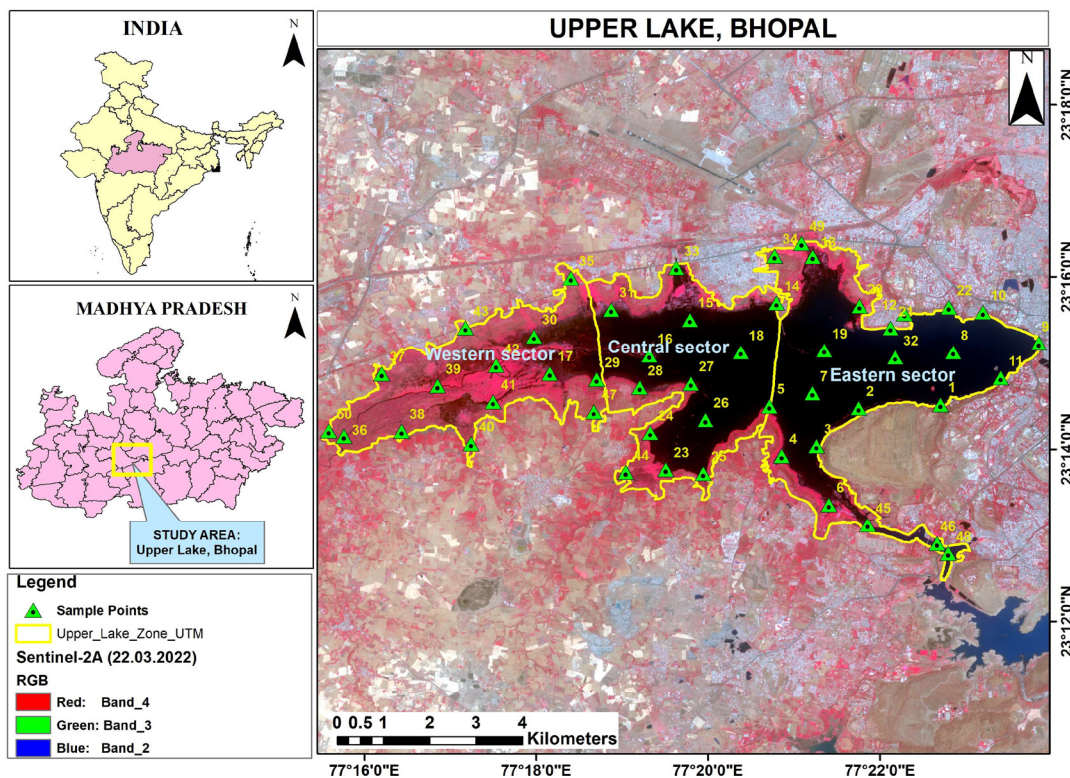


Fig. 1: Sentinel-2A false-color composite (FCC) image showing different sectors and sampling locations of the Upper Lake, Bhopal, India.

field sampling date, satellite images were acquired within a ± 3 -day window to ensure consistency between in situ and satellite observations. Priority was given to scenes with less than 10% cloud cover, and pre-monsoon and post-monsoon datasets were compiled for each year from 2013 to 2022. The reflectance values from the relevant bands, Blue (Band-2), Green (Band-3), Red (Band-4), and Near-Infrared (Band-5), were extracted for further analysis (Roy et al. 2016).

2.2.3 Image Preprocessing and Water Body Extraction

Before analyzing the reflectance-turbidity relationships, each Landsat image underwent a series of preprocessing steps. Using the Quality Assessment (QA_PIXEL) band provided by the USGS, clouds, cloud shadows, and snow pixels were masked to ensure that only valid reflectance values were retained. To isolate the Upper Lake's water surface, the Normalized Difference Water Index (NDWI) was calculated using the formula $NDWI = (Green - NIR) / (Green + NIR)$, as proposed by McFeeters (1996). A threshold value of $NDWI > 0.1$ was applied to generate a binary water mask, effectively separating water pixels from land, vegetation, and urban areas. This mask was used to clip reflectance values only for the open-water regions of the lake, minimizing background noise in the model calibration phase.

2.2.4 Turbidity Algorithm Development

To establish a relationship between in-situ turbidity and satellite-derived reflectance, a series of empirical regression models was tested. Each spectral band and selected band ratio (e.g., blue/red and green/red) were analyzed for correlation with the measured NTU values. Data points from coinciding

fieldwork and Landsat-8 OLI images were matched spatially, and linear, logarithmic, and exponential regression models were developed using OriginPro and SPSS. The band ratio of the blue band (Band-2) and red band (Band-4) consistently demonstrated the strongest correlation ($R^2=0.89$) with turbidity, which aligns with the findings of similar studies in Indian freshwater systems, where blue and red wavelengths showed maximum scattering from suspended sediments (Gholizadeh et al. 2016, Allam et al. 2020, Sharma et al. 2020). The final model was selected based on the highest coefficient of determination (R^2) and the lowest root mean square error (RMSE). The relationship between the band ratio of Landsat-8 OLI (Band-2: Band-4) and in-situ turbidity is shown in Fig. 2, and the derived equation is presented in Equation (1).

$$\text{Turbidity (NTU)} = 59.021 \times (\text{OLI B-2/OLI B-4}) - 40.42 \quad \dots(1)$$

The model was calibrated using training data from the field-satellite pairs and validated using an independent subset. The validation metrics included RMSE and R^2 , which confirmed the model's reliability across seasons and varying turbidity conditions.

3. RESULTS AND DISCUSSION

3.1 Seasonal Variation in Turbidity

This section presents the results of turbidity estimation derived from the calibrated remote sensing model based on Landsat-8 OLI Surface Reflectance data and validated using in-situ measurements. Table 1 shows the sector-wise *in situ* data collected from 50 selected sample locations in

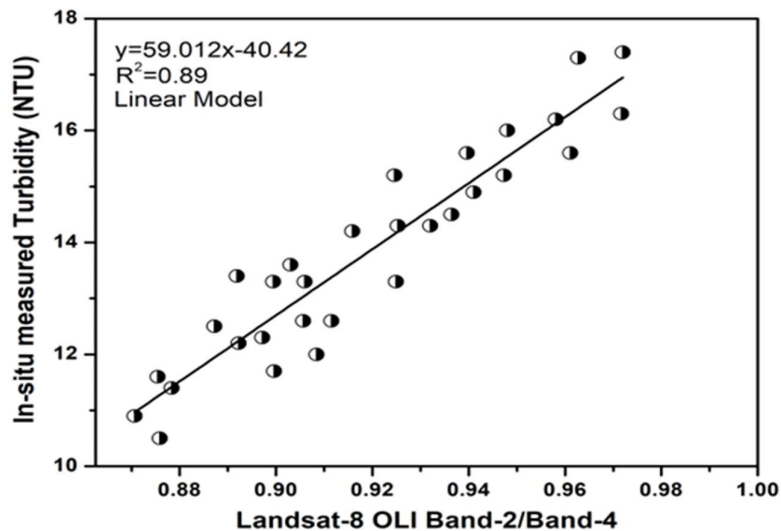


Fig. 2: Scatter plot showing the relationship between the in-situ turbidity measurements and Landsat-8 OLI band ratios.

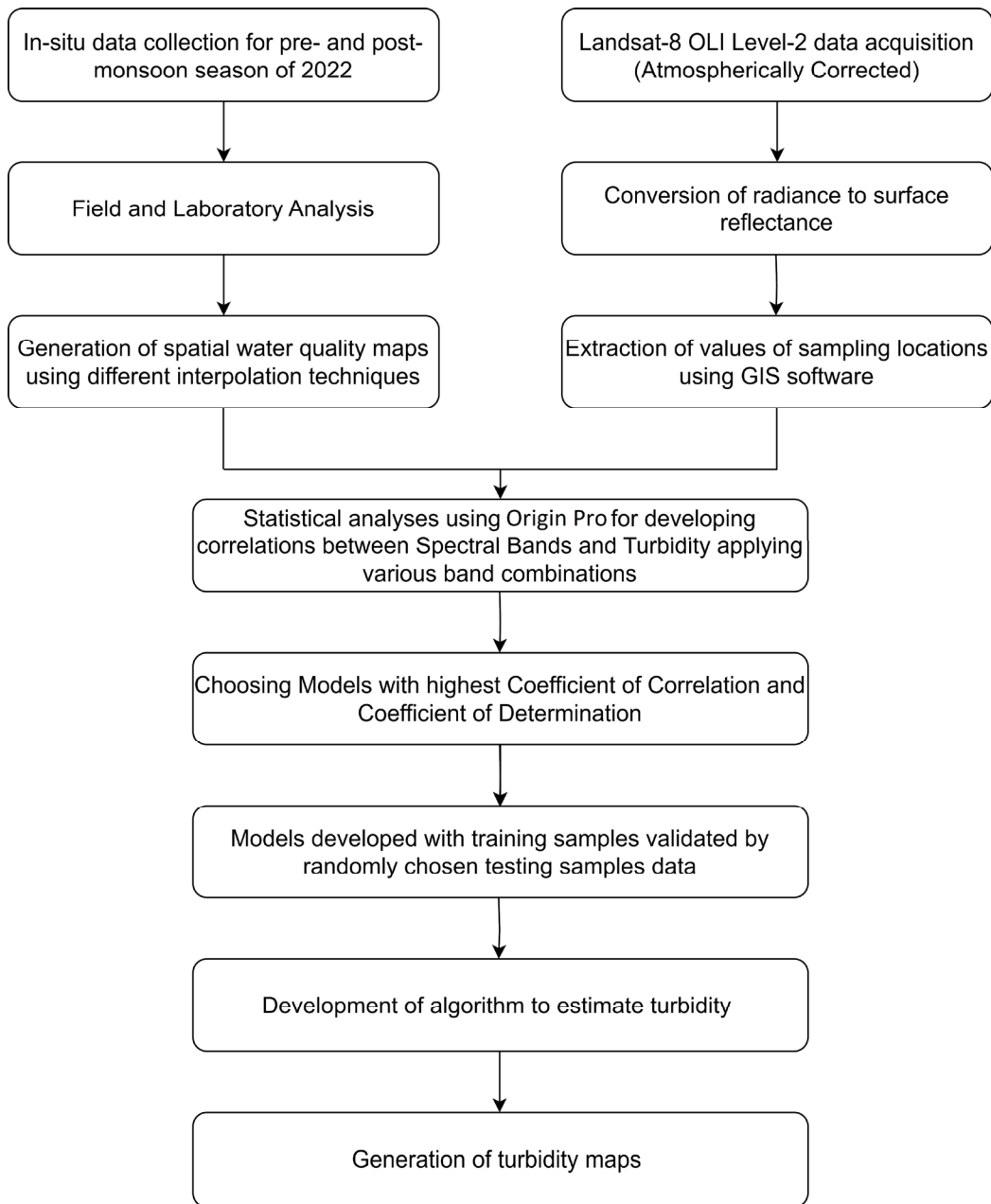


Fig. 3: Methodology flowchart for the estimation and generation of turbidity maps for Upper Lake, Bhopal.

Table 1: In-situ turbidity collected over the Upper Lake, Bhopal, during the pre- and post-monsoon seasons of 2022.

Turbidity [NTU]						
Pre-monsoon season-2022			Post-monsoon season-2022			
Sector	Minimum	Maximum	Average	Minimum	Maximum	Average
Eastern Sector	14.3	20.4	17.63	15.7	23.1	19.38
Central Sector	7.1	16.2	8.29	9.5	26.8	14.87
Western Sector	4.3	11.9	11.95	10.8	28.8	24.8

the Upper Lake, Bhopal, during the pre- and post-monsoon seasons of 2022.

In situ analysis revealed distinct seasonal fluctuations in turbidity levels across the lake during the 2022 observation period. During the pre-monsoon periods (April–June), turbidity values were generally lower, ranging between 4 NTU and 20 NTU, particularly in the central and deeper sections of the lake. These lower values are primarily attributed to minimal inflows, clear weather conditions, and sediment settling, as there was limited disturbance of the lake bed and relatively less surface runoff. In contrast, the post-monsoon periods (October–December) showed significantly elevated turbidity levels, with several locations exceeding 20 NTU. This sharp rise can be attributed to monsoonal runoff, which carries high loads of suspended solids, organic matter, and urban waste into the lake through open drains and inflow channels during the monsoon.

In the present study, satellite data were used to estimate the turbidity of the Upper Lake, Bhopal. Satellite-derived turbidity maps confirmed the presence of extensive sediment plumes, especially near urban drain outlets such as the Patra Nullah and Bairagarh inlet, aligning well with in-situ measurements and past studies (Durga Rao et al. 2009, Prasad & Tiwari 2019). From 2013 to 2022, the seasonal analysis of turbidity in the Upper Lake, Bhopal, revealed a consistent pattern of higher turbidity levels during the post-monsoon season than during the pre-monsoon period, with notable inter-annual variability influenced by rainfall intensity, urban runoff, and anthropogenic activities. During the pre-monsoon months (March–May), turbidity is generally moderate to high, reflecting limited inflow and sediment input, whereas post-monsoon months (October–November) consistently show elevated turbidity due to catchment runoff laden with sediments and organic matter following monsoon rains (Mishra & Prasad 2015). Spatial analysis using Landsat-8 OLI surface reflectance data revealed that areas near urban outfalls and drainage inlets exhibited persistently high turbidity values, indicating a direct influence from domestic and stormwater discharge.

In 2013, the baseline year of Landsat-8 availability, turbidity levels during both the pre- and post-monsoon seasons were high, with spatial concentrations near inflow zones, reflecting relatively stable catchment conditions. Fig. 4(a) shows relatively high turbidity (20 NTU) as compared to Fig. 4(b) (19 NTU). The average turbidity of the entire lake was 18.07 NTU and 14.45 NTU during the pre- and post-monsoon seasons of 2022, respectively. Fig. 4(c) shows that the ES of the lake is highly turbid water (18.07 NTU) compared to WS. However, high turbidity (14.34 NTU) was recorded in the CS and ES during the

post-monsoon season of 2014 (Fig. 4(d)). The ES remains at a high turbidity concentration throughout the year, which is mainly influenced by increasing construction activities, sewage discharge, and urban expansion around the lake's eastern periphery. Fig. 4(e) shows a similar pattern of turbidity as compared to Fig. 4(c) during the post-monsoon season. However, Fig. 4(f) demonstrates that the maximum area of the lake was under moderate to high turbidity during the post-monsoon period in 2015. The turbidity increased significantly, which is correlated with higher-than-average rainfall and sediment-rich runoff, as observed in similar studies across central Indian lakes (Mishra & Prasad 2015). The average turbidity was 11.96 NTU and 13.37 NTU during the pre- and post-monsoon seasons of 2015, respectively. Fig. 4(g) depicts high turbidity in the ES due to a prolonged dry spell, which caused reduced dilution and concentration of suspended solids (Sharma 2020). Fig. 4(h) shows that the turbidity value of the entire lake was moderate owing to a weak monsoon year. The average turbidity concentration of the entire lake was 11.73 NTU and 14.46 NTU during the pre- and post-monsoon seasons of 2016, respectively. Fig. 4(i) shows that ES and CS experience high turbidity (20 NTU) compared to WS (3.8 NTU). Fig. 4(j) depicts a moderate pattern of post-monsoon turbidity, 18.25 NTU, which is recorded particularly near the southeast inflow regions, attributed to intense rainfall and unregulated urban discharge, aligning with similar findings by Farooq et al. (2021). In 2018 (Fig. 4(k) and (l)), a declining pattern of turbidity levels was observed for both seasons, except for the ES and CS of the lake, owing to a drier monsoon and partial implementation of catchment management under the Bhopal Lake Conservation Scheme (Sharma 2020). The average turbidity concentration of the lake was 10.77 NTU and 12.12 NTU during the pre- and post-monsoon seasons of 2018, respectively.

Fig. 4(m) shows the lake water turbidity of the pre-monsoon season of 2019, which slightly declined from the similar pattern of the pre-monsoon season of 2018. Fig. 4(n) depicts ES and WS showing high turbidity concentration (17.3 NTU), except for the maximum pockets of CS. The average turbidity of the lake was 10.12 NTU and 11.66 NTU during the pre- and post-monsoon seasons, respectively. Fig. 4(o) and (p) show a similar pattern of turbidity concentration during the pre- and post-monsoon seasons of 2020. The average turbidity of the lake was 7.18 NTU and 9.6 NTU during the pre-monsoon and post-monsoon seasons, respectively. Similarly, Fig. 4(q) and (r) show the pre- and post-monsoon turbidity patterns of 2021. The average turbidity values were 7.87 NTU and 10.57 NTU during the pre- and post-monsoon seasons, respectively. From the overall observation, it was found

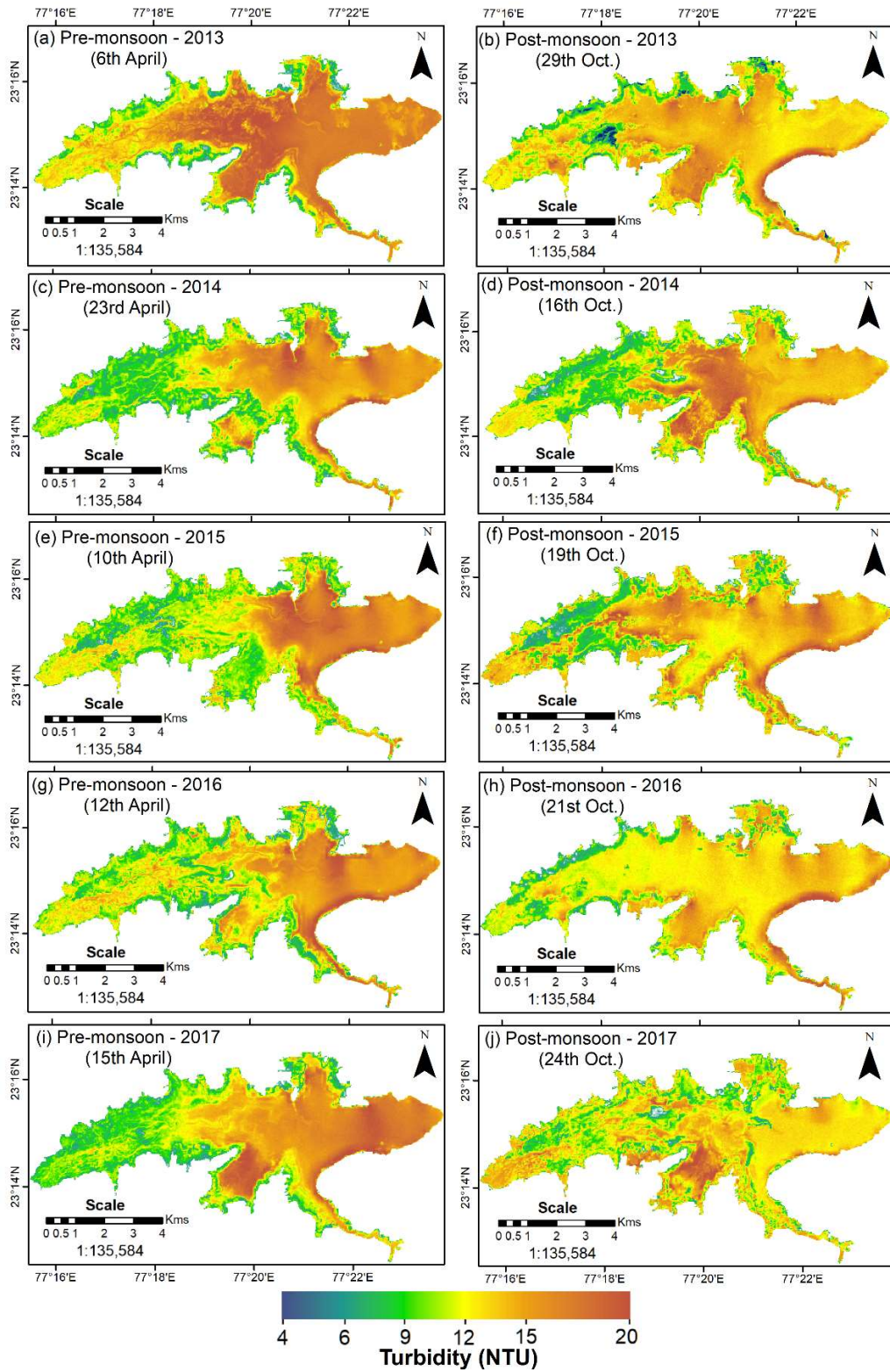


Fig. 4 (a-j): Turbidity images from Landsat-8 OLI bands during the pre- and post-monsoon seasons from 2013 to 2017.

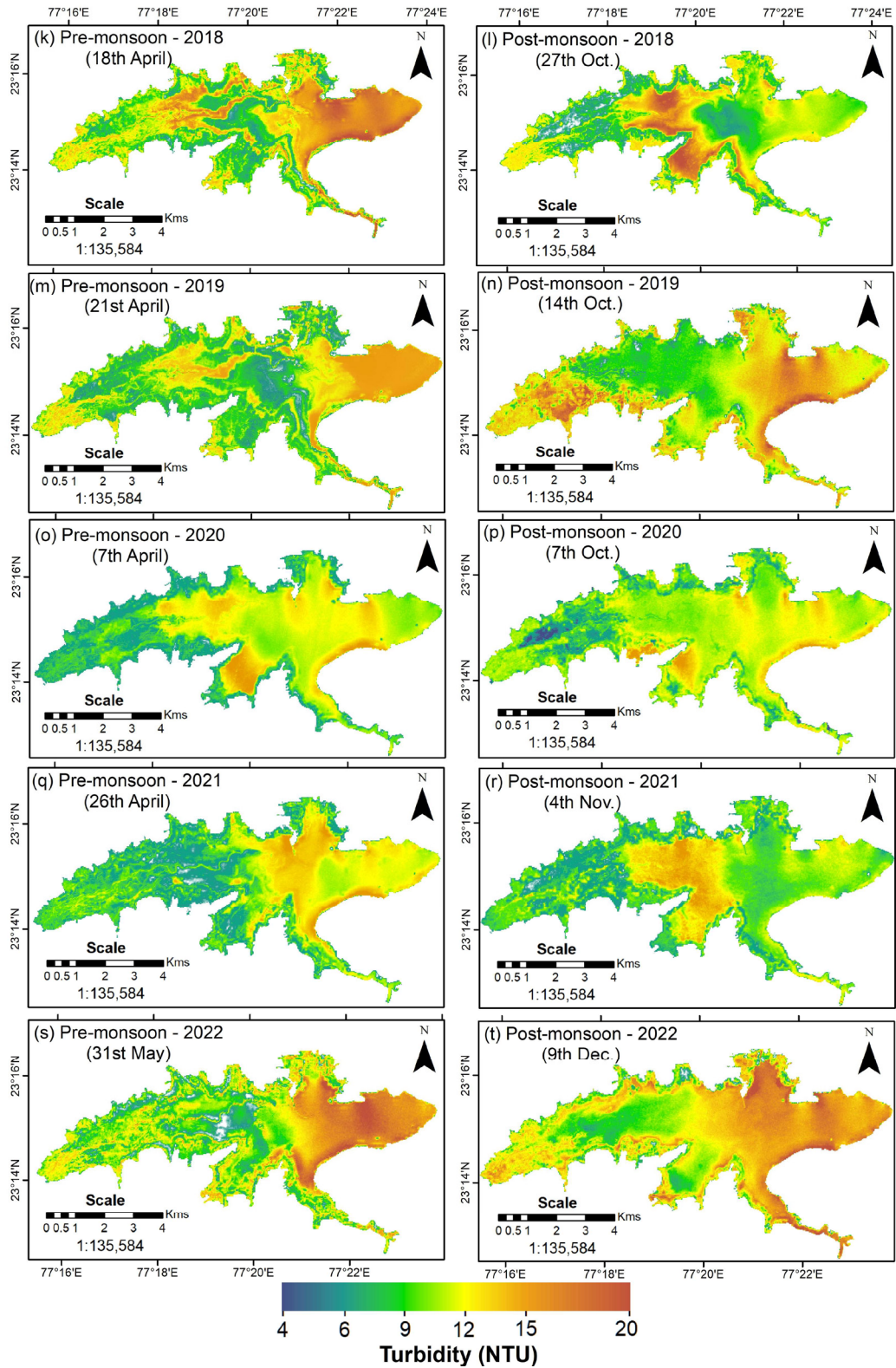


Fig. 4 (k-t): Turbidity images from Landsat-8 OLI bands during the pre- and post-monsoon seasons from 2018 to 2022.

that the distribution of turbidity was more or less the same in the pre- and post-monsoon season of 2020-21. The above-mentioned period exhibited a unique scenario, where both seasonal turbidity levels were markedly low. This may be attributed to the COVID-19 lockdown, which reduced human-induced activity, boating, and industrial effluent discharge, a phenomenon echoed in water bodies globally (Sharma & Gupta 2022). Finally, 2022 offered the most detailed insight because of concurrent in-situ sampling. Fig. 4(s) shows that the ES experienced relatively high turbidity (20 NTU) compared to the WS (12.13 NTU) and CS (14.54 NTU) of the lake. Fig. 4(t) shows that the entire lake has a maximum turbidity concentration (19.67 NTU), except for some pockets of CS (14.54 NTU) and WS (15.27 NTU), highlighting the continued influence of runoff and sediment-laden flows, particularly near the Shahpura and Bairagarh catchments (Talwar et al. 2014). The satellite-derived turbidity model, based on the Band-2/Band-4 ratio, showed excellent agreement ($R^2 = 0.89$) with field data for 2022, supporting its robustness for multi-year monitoring (Joshi & Agrawal 2022). Overall, the decade-long analysis confirmed a consistent seasonal pattern of moderate to high turbidity during the pre-monsoon season and high turbidity during the post-monsoon season, with year-to-year variability driven by rainfall, urban growth, and local interventions. These findings emphasize the value of combining satellite observations with ground-truthing for long-term lake water quality assessment in rapidly urbanizing landscapes.

3.2 Comparison of Sector-wise Average Turbidity (2022)

A comparison of the average values of in-situ turbidity

measurements at different sectors during the pre- and post-monsoon seasons of 2022 is shown in Fig. 5. The figure shows that the post-monsoon season experienced higher turbidity than the pre-monsoon season. During the pre-monsoon season of 2022, the average value of turbidity was found in WS (11.95 NTU), CS (8.29 NTU), and ES (17.63 NTU). Similarly, during the post-monsoon season of 2022, the average turbidity values were observed in WS (21.83 NTU), CS (14.87 NTU), and ES (19.38 NTU). The in-situ turbidity measurements revealed that the WS experienced maximum turbidity during the post-monsoon season, whereas the ES experienced maximum turbidity during the pre-monsoon season of 2022. However, the CS remains low in terms of turbidity throughout the year. Fig. 6 depicts the sector-wise distribution of average turbidity derived from Landsat-8 OLI during the pre-monsoon and post-monsoon seasons of 2022. This shows that the post-monsoon season experiences higher turbidity than the pre-monsoon season. During the pre-monsoon season of 2022, the average turbidity values were estimated at WS (7.76 NTU), CS (7.15 NTU), and ES (9.82 NTU). Similarly, during the post-monsoon season of 2022, the average value of turbidity is estimated in WS (14.26 NTU), CS (13.99 NTU), and ES (15.5 NTU). The analysis of Fig. 5 and 6 indicates that the average in-situ observed turbidity pattern agrees well with Landsat-8 OLI-derived turbidity.

3.3 Inter-Annual Trends (2013–2022)

In the present study, the dynamic nature of inter-sectoral and seasonal changes in the turbidity of the Upper Lake, Bhopal, was studied, which is mainly influenced by various

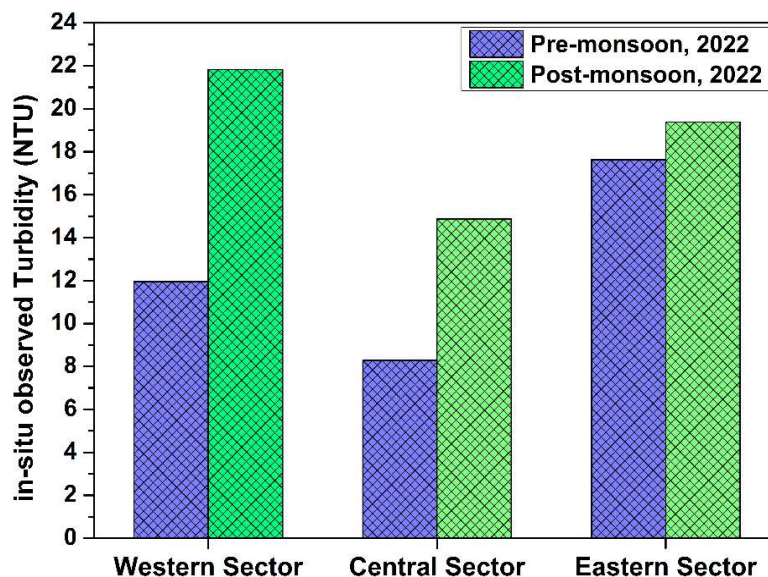


Fig. 5: Comparison of average turbidity at different sectors from in-situ measurements during the pre- and post-monsoon seasons of 2022.

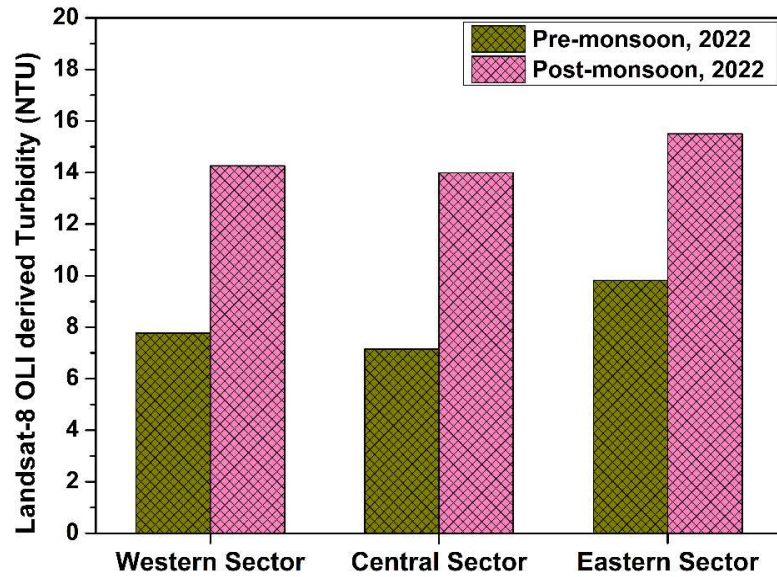


Fig. 6: Comparison of average turbidity in different sectors derived from Landsat-8 OLI during the pre- and post-monsoon seasons of 2022.

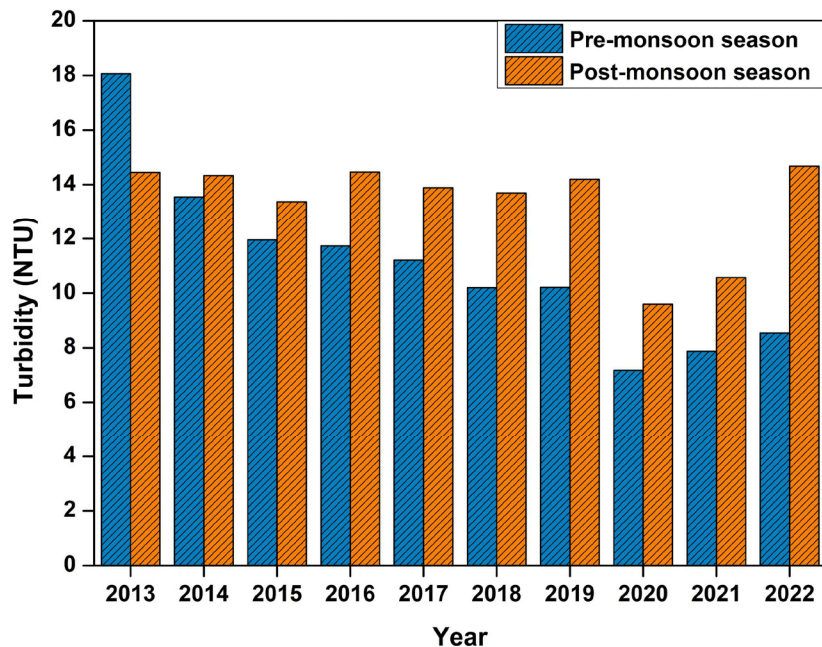


Fig. 7: Comparison of average turbidity derived from Landsat-8 OLI during the pre- and post-monsoon seasons from 2013 to 2022.

anthropogenic activities. A comparison of the pre- and post-monsoon season average values of the turbidity of the entire lake estimated from satellite data from 2013 to 2022 is shown in Fig. 7. Long-term analysis revealed that the average turbidity during the post-monsoon season was higher than that during the pre-monsoon season, except for 2013. From 2014 to 2019, most areas of the lake showed high turbidity (10.2 – 18.07 NTU), with exceptions limited to localized

high-inflow zones. However, in 2020 and 2021, there was marked moderate turbidity (7.18 – 10.57 NTU) due to the COVID-19 lockdown. The post-COVID-19 period showed a marked expansion of high turbidity (8.54 – 14.68 NTU), indicating escalating sedimentation and pollutant loading.

This trend corresponds to increased urbanization, construction activities, and land-use changes in the lake's catchment area. The northeastern and western peripheries,

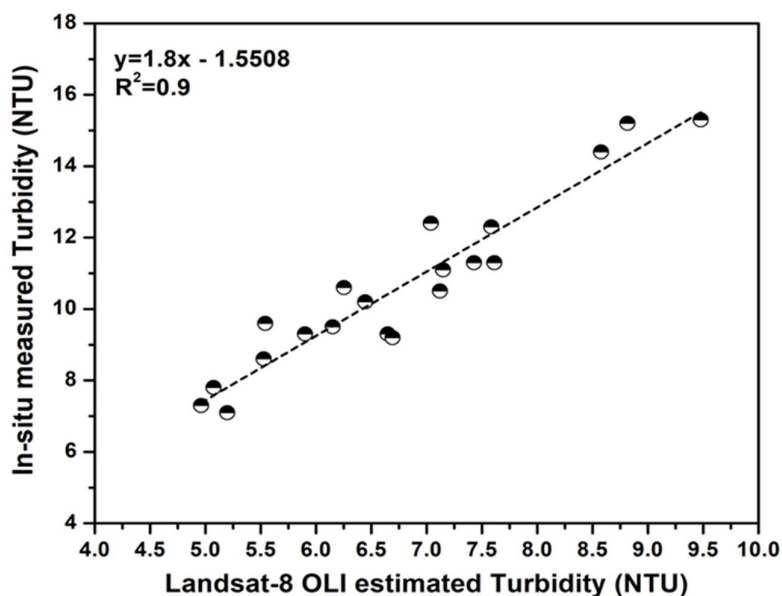


Fig. 8: Scatter plot showing the relationship between in-situ observed turbidity and Landsat-8 OLI estimated turbidity.

which have witnessed dense residential and commercial development and river run-off, emerged as zones with persistently high turbidity. The lack of effective stormwater management and wastewater treatment infrastructure appears to be a major driver of turbidity escalation. These findings mirror those of other urban lake studies in India, where land disturbance and catchment degradation directly influenced water clarity (Rather & Dar 2020).

3.4 Validation of Turbidity Retrieval Model

Turbidity was estimated for the pre- and post-monsoon seasons using Landsat-8 Operational Land Imager (OLI) images for the Upper Lake, Bhopal. The turbidity retrieval model developed using the Landsat-8 OLI band ratio of blue and red band reflectance and calibrated with in-situ measurements showed a strong correlation. The model yielded a coefficient of determination (R^2) of 0.9 and a Root Mean Square Error (RMSE) of ± 4.04 NTU during validation (Fig. 8). These metrics indicate the high reliability of the model in capturing actual turbidity variations across seasons and locations. The model was particularly effective in estimating turbidity within the range of 5–50 NTU. However, at very high turbidity levels (>60 NTU), there was a slight tendency to underestimate values, likely due to reflectance saturation in the red band, which limits the differentiation of dense sediment loads. Such limitations have also been noted in similar studies using optical sensors such as Landsat and Sentinel (Nechad et al. 2010, Gholizadeh et al. 2016).

4. CONCLUSIONS

This study successfully demonstrated the integration of satellite remote sensing and in-situ turbidity measurements for monitoring water quality in the Upper Lake, Bhopal, over a decadal time frame (2013–2022) during the pre- and post-monsoon seasons. Using Landsat-8 OLI Surface Reflectance data calibrated against the obtained field data, an empirical model was developed to retrieve turbidity with high spatial and seasonal variation. The model achieved strong validation results ($R^2 = 0.89$), establishing its suitability for ongoing and future water quality assessments of Lake Taal. The findings revealed significant seasonal and interannual variations in the turbidity. Post-monsoon seasons consistently exhibit higher turbidity levels owing to increased runoff, urban drainage, and sediment inflow. Meanwhile, the pre-monsoon periods showed comparatively clearer water, suggesting a seasonal self-recovery potential. However, a gradual increase in turbidity across several sectors of the lake, especially near urban inflow points, indicates growing anthropogenic pressure, particularly from urban expansion, waste discharge, and unregulated changes in catchment areas. Spatial analysis identified persistent turbidity hotspots along the western and northeastern lake margins, highlighting the role of point and non-point source pollution. These areas require targeted interventions, such as drainage management, constructed wetlands, and pollution control measures. In contrast, the central sector of the lake maintained relatively low turbidity owing to better protection and minimal human interference, underscoring the value of

riparian buffers and regulated land use. This study provides a cost-effective and scalable methodology for long-term water quality monitoring and generates critical geospatial intelligence that can support lake management policies and Ramsar site conservation strategies. The approach adopted here is replicable for similar water bodies across India and other developing regions, especially where conventional monitoring is limited by resource availability. Going forward, the integration of higher-resolution sensors (e.g., Sentinel-2 MSI), Machine Learning Models, and multi-parameter water quality indices can further enhance the accuracy and scope of monitoring. Regular data-driven surveillance, combined with community involvement and government action, is essential for restoring and safeguarding the ecological health of Upper Lake, Bhopal, and fulfilling its role as a critical urban wetland under the Ramsar Convention.

5. ACKNOWLEDGMENTS

The authors are grateful to the Vice Chancellor of Gangadhar Meher University, Sambalpur, for providing all the support and encouragement. Special thanks to Dr. Abhilasha Bhawsar, Assistant Professor, Department of Environmental Sciences and Limnology, Barkatullah University, Bhopal, for providing essential support and laboratory facilities to conduct the research.

6. REFERENCES

- Allam, M., Yawar Ali Khan, M. and Meng, Q., 2020. Retrieval of turbidity on a spatio-temporal scale using Landsat 8 SR: a case study of the Ramganga river in the Ganges basin, India. *Applied Sciences*, 10(11), pp.1-15. [DOI]
- Bilotta, G.S. and Brazier, R.E., 2008. Understanding the influence of suspended solids on water quality and aquatic biota. *Water Research*, 42(12), pp.2849-2861. [DOI]
- Brezonik, P., Menken, K.D. and Bauer, M., 2005. Landsat-based remote sensing of lake water quality characteristics, including chlorophyll and colored dissolved organic matter (CDOM). *Lake and Reservoir Management*, 21(4), pp.373-382. [DOI]
- Chen, M. and Chen, F., 2017. Effect of suspended solids on interaction between filter-feeding fish *Aristichthys nobilis* and zooplankton in a shallow lake using a mesocosm experiment. *Journal of Freshwater Ecology*, 32(1), pp.219-227. [DOI]
- Central Pollution Control Board (CPCB), 2019. "Status of Water Quality in India – 2019." Retrieved June 25, 2024, from <https://cpcb.nic.in/nwmp-data-2019/>
- Das, A., Regin, J.J., Suhasini, A. and Lisa, K.B., 2024. Study on spatial variations of surface water quality vulnerable zones in Baitarani River basin, Odisha, India. *Nature Environment and Pollution Technology*, 23(1), pp.33-53. [DOI]
- Dekker, A.G., Vos, R.J. and Peters, S.W.M., 2002. Analytical algorithms for lake water TSM estimation for retrospective analyses of TM and SPOT sensor data. *International Journal of Remote Sensing*, 23(1), pp.15-35. [DOI]
- Durga Rao, K.H.V., Singh, A.K. and Roy, P.S., 2009. Study of morphology and suspended sediment of Bhopal Upper Lake using spatial simulation technique and remote sensing data. *Journal of the Indian Society of Remote Sensing*, 37, pp.433-441. [DOI]
- Everard, M., Ahmed, S., Gagnon, A.S., Kumar, P., Thomas, T., Sinha, S., Dixon, H. and Sarkar, S., 2020. Can nature-based solutions contribute to water security in Bhopal? *Science of the Total Environment*, 723, pp.1-15. [DOI]
- Farooq, S., Shrivastava, P. and Bhat, M.H., 2021. Water quality assessment of Upper Lake Bhopal with reference to conservation and management. *EPRA International Journal of Multidisciplinary Research*, 7(9), pp.328-333. [DOI]
- Gholizadeh, M.H., Melesse, A.M. and Reddi, L., 2016. A comprehensive review on water quality parameters estimation using remote sensing techniques. *Sensors*, 16(8), pp.1-15. [DOI]
- Jally, S.K., Mishra, A.K. and Balabantaray, S., 2021. Retrieval of suspended sediment concentration of the Chilika Lake, India using Landsat-8 OLI satellite data. *Environmental Earth Sciences*, 80, pp.1-15. [DOI]
- Joshi, A. and Agrawal, S., 2022. Reduction in turbidity of Indian lakes through satellite imagery during COVID-19 induced lockdown. *Spatial Information Research*, 30, pp.715-727. [DOI]
- Maity, S., Maiti, R. and Senapati, T., 2022. Evaluation of spatio-temporal variation of water quality and source identification of conducive parameters in Damodar River, India. *Environmental Monitoring and Assessment*, 194, pp.1-15. [DOI]
- McFeeters, S.K., 1996. The use of the normalized difference water index (NDWI) in the delineation of open water features. *International Journal of Remote Sensing*, 17, pp.1425-1432. [DOI]
- Mishra, D.R. and Prasad, A., 2015. Spatiotemporal patterns of turbidity in inland waters using remote sensing. *Journal of Hydrology*, 527, pp.713-727. [DOI]
- Nechad, B., Ruddick, K. and Park, Y., 2010. Calibration and validation of a generic multisensor algorithm for mapping turbidity in coastal waters. *Remote Sensing of Environment*, 114(4), pp.854-866. [DOI]
- Pahlevan, N., Sarkar, S., Franz, B.A., Balasubramanian, S.V. and He, J., 2017. Sentinel-2 Multispectral Instrument (MSI) data processing for aquatic science applications: demonstrations and validations. *Remote Sensing of Environment*, 201, pp.47-56. [DOI]
- Parashar, C., Verma, N., Dixit, S. and Shrivastava, R., 2008. Multivariate analysis of drinking water quality parameters in Bhopal, India. *Environmental Monitoring and Assessment*, 140, pp.119-122. [DOI]
- Prasad, B. and Tiwari, H.L., 2019. Sedimentation analysis and remedial measures for Upper Lake Bhopal using remote sensing and GIS. *International Journal of Innovative Technology and Exploring Engineering (IJITEE)*, 8(5), pp.1008-1013.
- Ramsar Sites Information Service, 2024. "Bhoj Wetland Ramsar Information Sheet." Retrieved June 25, 2024, from <https://rsis Ramsar.org>
- Rather, H.A. and Gautam, V., 2023. A study of winter avifaunal diversity in Upper Lake, in the city of Bhopal, Madhya Pradesh, India. *Journal of Animal Diversity*, 5(4), pp.48-56. [DOI]
- Rather, I.A. and Dar, A.Q., 2020. Assessing the impact of land use and land cover dynamics on water quality of Dal Lake, NW Himalaya, India. *Applied Water Science*, 10, pp.1-15. [DOI]
- Roy, D.P., Zhang, H.K., Ju, J., Gomez-Dans, J.L., Lewis, P.E., Schaaf, C.B., Sun, Q., Li, J., Huang, H. and Kovalskyy, V., 2016. A general method to normalize Landsat reflectance data to nadir BRDF adjusted reflectance. *Remote Sensing of Environment*, 176, pp.255-271. [DOI]
- Sharma, S. and Gupta, A., 2022. Impact of COVID-19 on water quality index of river Yamuna in Himalayan and upper segment: analysis of monsoon and post-monsoon season. *Applied Water Science*, 12(6), pp.1-15. [DOI]
- Sharma, S., 2020. Behavioral study of urban watersheds in Bhopal-city of lakes. *International Journal of Hydrology*, 4(3), pp.111-115. [DOI]
- Sharma, R., Kumar, R., Satapathy, S.C., Ansari, N.A., Singh, K.K., Mahapatra, R.P., Agarwal, A.K., Le, H.V. and Pham, B.T., 2020. Analysis of water pollution using different physicochemical parameters: a study of Yamuna River. *Frontiers in Environmental Science*, 8, pp.1-15. [DOI]

- Talwar, R., Agrawal, S., Bajpai, A. and Malik, S., 2014. Effect of catchment area activities on the physicochemical characteristics of water of Upper Lake, Bhopal with special reference to nitrate and phosphate concentration. *Current World Environment*, 9(1), pp.188-191. [DOI]
- UNESCO, 2018. "UN World Water Development Report 2018: Nature-Based Solutions for Water." Retrieved June 25, 2024, from <https://www.unwater.org/publications/world-water-development-report-2018>
- Wen, Z., Wang, Q., Liu, G., Jacinthe, P., Wang, X., Lyu, L., Tao, H., Ma, Y., Duan, H., Shang, Y., Zhang, B., Du, Y., Du, J., Li, S., Cheng, S. and Song, K., 2022. Remote sensing of total suspended matter concentration in lakes across China using Landsat images and Google Earth Engine. *ISPRS Journal of Photogrammetry and Remote Sensing*, 187, pp.61-78. [DOI]
- Yang, H., Kong, J., Hu, H., Du, Y., Gao, M. and Chen, F., 2022. A review of remote sensing for water quality retrieval: progress and challenges. *Remote Sensing*, 14(8), pp.1-15. [DOI]